A low-cost instrument for environmental particulate analysis based on optical scattering

Anna Morpurgo, Federico Pedersini, and Alessandro Reina
Department of Information Science, Università degli studi di Milano
Via Comelico 39/41, I–20135 Milano, Italy
e-mail: {anna.morpurgo, federico.pedersini, alessandro.reina}@unimi.it

***Abstract*—This paper presents the design, realization and calibration of a portable instrument for real-time measurement (concentration and size distribution) of airborne dust particles. The measuring principle is the estimation of the light scattered by the particles under illumination. The proposed design is characterized by low hardware cost and simplicity of calibration but, nevertheless, it delivers significant performance in terms of size resolution. This result could be achieved by means of an accurate processing of the detected signal, which maximizes the signal/noise ratio in detecting the scattering peaks. In order to get this signal processing chain running in real time on a low-cost platform (an ARM7-based microcontroller board), computationally efficient algorithms have been developed for optimal filtering and peak detection. For the metrological calibration of the instrument, a simple method is proposed, which employs commonly available materials with known particle size distribution, instead of expensive monodispersed test particles. The experimental results show the effectiveness of the proposed calibration and the ability of the instrument to reach a sensitivity and a granulometric resolution comparable to those of more sophisticated instruments.**

I. Introduction

In the field of environmental monitoring, instruments able to count and determine the size of airborne particulate matter are becoming increasingly important, besides the classical instruments measuring the particulate concentration in weight per volume unit. Recent studies [2] evidenced how the size distribution (granulometric analysis) of dust particles is even more informative than the total dust concentration in weight (gravimetric analysis), when investigating the incidence of negative effects on human health. The environmental research community has standardized the granulometric classification of dust [9], defining as *inhalable fraction* the particles with less than $100\ \mu\mathrm{m}$ diameter, *thoracic fraction* (PM_{10}) the particles under $10\ \mu\mathrm{m}$, and *breathable fraction* ($\mathrm{PM}_{2.5}$) for particles under $2.5\ \mu\mathrm{m}$.

Several techniques can be exploited to measure the concentration and the size distribution of particulate in environmental dust. Among them, optical scattering is generating increasing interest, mainly due to the possibility of building simple and compact instruments and the ability of such instruments to provide real-time measurements (in spite of gravimetric methods, giving only off-line results). The physical phenomenon exploited by this instrument is optical scattering: the airborne particles flowing across a thin red laser beam scatter the incident light; the scattered light reaches an optical detector, which generates a current pulse proportionally to the received light intensity. Each particle generates a signal peak, whose amplitude mainly depends on the particle size. If the relationship between scattered light power and particle size is invertible, it is possible, through a proper calibration, not only to count the particles, but also to evaluate their size.

This paper presents the design and construction of a portable instrument measuring the concentration and size distribution of airborne dust particles. The main goal of this design was to obtain a simple and inexpensive instrument which could, nevertheless, yield accurate measurements. This goal has lead, on one hand, to the effort of keeping the hardware cost low, by adopting a simple microcontroller platform. This choice has made it necessary to develop very efficient algorithms for the real-time processing of the detected signal, due to the limited computing power. On the other hand, a calibration procedure has been studied, which exploits commonly available materials as test particulate, and does not need any particular calibration equipment, instead of using monodispersed test particles, which are very expensive and need complex laboratory setups for being employed in calibration (e.g. chambers with controlled dust concentration).

The paper is organized as follows: in the next section, the physical principles of the measurement process are described; Section III presents both the hardware (the architecture) and software (the signal processing algorithms) aspects of the instrument, while Section IV describes the calibration procedure and the obtained experimental results.

II. Measurement Principle

The scattering of electromagnetic radiation by particles whose size is similar to the wavelength is exactly described by Mie's theory, representing the analytical solution of Maxwell's equations for particles interacting with electromagnetic waves in a homogeneous and isotropic medium [3], [4]. The intensity I of the scattered light is a function $f(\lambda, d, n, \theta)$ of the wavelength λ, the particle's diameter d, the refractive index n, and the scattering angle θ.

The curves presented in Figure 1 are computed for refraction indexes ranging from $1.55 + 0.5i$ (the index of diesel exhaust particles), to $2 + 0.5i$, which is the range of most particulate in urban environments [2], [5].

As Figure 1 shows, the intensity of the scattered light is mainly a monotonic function of the particle diameter and

978-1-4577-1772-7/12/$26.00 ©2012 IEEE

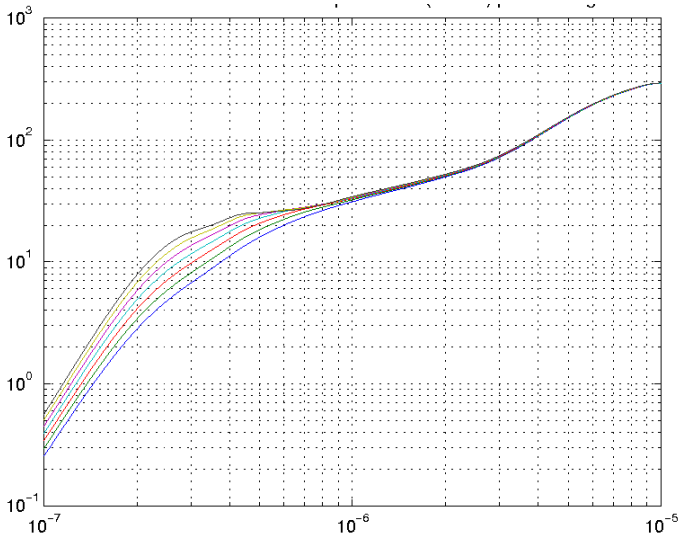

Fig. 1. Mie's solution for the light intensity ($\lambda = 0.65\,\mu\text{m}$) scattered orthogonally to the incident light direction, as a function of the particle size, for different refractive indexes (ranging from $1.5 + 0.5i$ to $2 + 0.5i$) (X: particle diameter in µm, Y: squared root of the intensity)

depends slightly on the refractive index; in particular, for diameters above $1\,\mu\text{m}$ the intensity depends only on the particle size. This makes the function a means to estimate the particle size from a measure of the scattered light intensity.

More generally [1], defining the *size parameter* $x = \frac{2\pi\ r}{\lambda}$, when $x \ll 1$ (thas is, the particle size is much smaller than the wavelength), Mie's formulation converges to Rayleigh scattering, whereby the scattered intensity is proportional to r^6. Viceversa, for $x \gg 1$, the scattered intensity is proportional to r^2. The point $x = 1$ can be therefore considered the transition point between Rayleigh and Mie scattering. In the case considered in Fig. 1, $x = 1$ corresponds to a particle diameter $D = 2r = \frac{\lambda}{\pi} \approx 0.2\,\mu\text{m}$.

III. The Instrument

The overall structure of the instrument is schematized in Figure 2. The sampled air flows through a sensing chamber, in which a collimated laser beam illuminates the air flow. The airborne dust particles scatter the incident light in all directions, and a fraction of the scattered light reaches the sensing photodiode. The current generated by the photodiode is amplified, converted to digital and processed by the computing system, responsible for signal processing, instrument control and user interface. In the following sections, the structure of the sensing chamber and the proposed processing algorithm are described in details.

A. The Optical Sensor

The sensor consists of a dark chamber in which the sampled air flows through a cylindrical duct, as shown in Figure 2 (left). The air flow is regulated by a constant-flow pump and the duct is structured in such a way to ensure that the flow along the duct is laminar, with constant velocity. Inside the chamber, the air flow is crossed by a collimated laser beam,

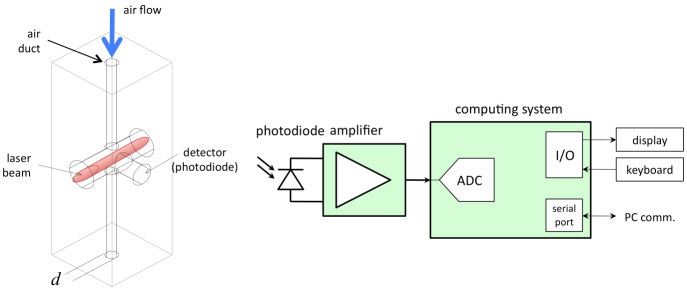

Fig. 2. (left) Structure of the sensing chamber. The observation volume corresponds to the intersection of the cylindric air flow with the laser beam. (right) Structure of the instrument. A fraction of the scattered light reaches the photodiode, which converts light intensity into current. The photodiode signal is amplified, converted to digital and processed by the computing system.

which is generated by a red laser diode ($\lambda = 0.65\,\mu\text{m}$). The diameter of the collimated beam is slightly wider than that of the cylindrical air column, thus ensuring that the totality of the sampled air is illuminated during the transit.

The observation volume corresponds to the intersection of the air flow with the laser beam, both of which are circular in section. Since our aim is to measure the size of the particulate, it must be assumed that at most one particle crosses the observation volume at a time. This poses a limit on the maximum concentration of dust, in term of number of particles per volume unit. As figure 2 shows, the diameter of the air duct $d = 2.4\,\text{mm}$, while the width of the light beam $w_l \approx 3\,\text{mm}$. This corresponds to an observation volume $V_{obs} \approx \pi \frac{d^2}{4} w_l = 3.4\,\text{mm}^3$. The maximum concentration is therefore:

$$C_{max} = \frac{1}{V_{obs}} \approx 3 \cdot 10^8\ \frac{\text{particles}}{\text{m}^3}$$

which is largely more than the typical concentration of particulate in urban environments, thus making the instrument suited for urban dust monitoring applications [2].

The sensing element, a high-sensitivity photodiode, is placed at the end of a cylindrical duct whose axis is orthogonal to both the laser beam and air flow direction, in order to collect the light scattered perpendicularly to the incident light direction. The distance between the photosensor and the illuminated observation volume is $20\,\text{mm}$, so that the particle-detector distance lies in the range $20 \pm 1.2\,\text{mm}$ ($\pm 6\%$). This distance keeps the influence of the particle-detector distance in the detected light intensity to a reasonably low amount (approx. $\pm 12\%$).

The signal from the photodiode is amplified by a transimpedance preamplifier. The circuit of the developed amplifier is presented in figure 3. The photodiode is polarized in photovoltaic mode, to maximize the amplifier's sensitivity and linearity. Instead of a traditional FET-input operational amplifier, a CMOS op-amp has been chosen for this design because, besides the necessary very high input impedance ($10^{13}\,\Omega$), it can operate with low-voltage single power supply ($3\,\text{V}$), like the rest of the circuitry, thus allowing to reduce the hardware cost. The gain of the amplifier, determined by

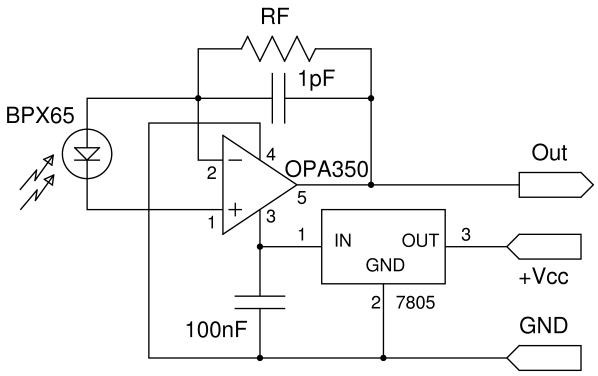

Fig. 3. Schematics of the developed photodiode preamplifier. The photodiode is connected in photovoltaic configuration, to optimize sensitivity and linearity.

the feedback resistor R_F, has been adjusted experimentally, in order to cover the desired measurement range.

B. Signal Acquisition and Processing

In order to minimize the hardware cost, for the implementation of the computing system we adopted a microcontroller from Analog Devices (ADuC7020), containing an ARM7 core and all the needed peripherals (internal Flash/RAM memory for program and data, A/D converter, I/O lines, UART).

The signal produced by the amplifier is acquired and converted to digital by means of the internal A/D converter of the microcontroller, a 12-bit SAR converter. The determination of the correct sampling frequency of the photodiode signal has to consider the shape of the pulses generated by the particle crossing the observation volume. On a first approximation, a rectangular pulse can be expected, whose duration depends on the air velocity in the duct $v_a = P/S_d$, being $S_d = \pi(d/2)^2$ the duct section and P the constant air flow maintained by the pump. The pulse duration is therefore:

$$T_p = \frac{w_l}{v_a} = \frac{\pi}{4}\frac{w_l \cdot d^2}{P}.$$

The pump has been adjusted to an air flow $P = 0.7\,\mathrm{l/min}$, yielding a pulse duration $T_p = 291\,\mu\mathrm{s}$. In order to reliably detect the pulses and accurately evaluate their amplitude, they should last over a sufficient number of samples. We imposed a minimum of 10 samples within a peak, yielding a maximum sampling period $T_s = T_p/10 = 29.1\,\mu\mathrm{s}$, which corresponds to a minimum sampling frequency $f_{s,min} = 1/T_s = 34.4\,\mathrm{kHz}$. Having to choose among the admissible sampling frequencies of the A/D converter, we set $f_s = 37\,\mathrm{kHz}$.

Ideally, the shape of the pulses should be rectangular, as their shape describes the time function of the energy collected by the photodiode as the particle crosses the laser beam. Figure 4 presents an example of the signal acquired by the system (blue solid-dotted line). The peak represents a typical response to the detection of a particle; the pulse deviates from the ideally expected rectangular shape by the presence of significant smoothing and a negative overshoot. The causes for

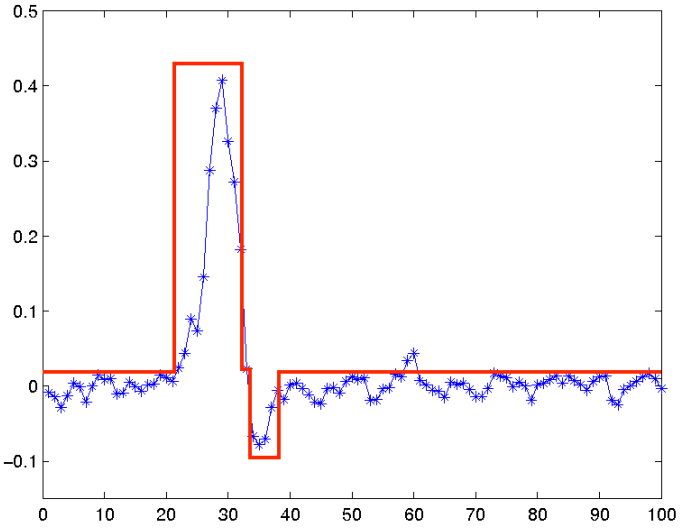

Fig. 4. The blue line represents an example of the acquired signal from the sensor ($f_s = 37\,\mathrm{kHz}$). The peak represents the response to the detection of a particle. The red line represents the approximation of the pulse with two rectangular pulses.

this deviation are mainly two: the spatial distribution of the beam intensity varies across its section (it declines towards the beam boundary), resulting in a smoothing of the pulse's rising and falling edges. Further signal smoothing and the overshooting can be ascribed to the transfer function of the photodiode amplifier. However, it is important to notice that both these effects can be described as a convolution on the photodiode signal, like a linear filter. Therefore, they only change the final shape of the pulse, but not its amplitude, which remains, as in the ideal case, a monotonic function of the particle size.

According to the principles of optimal detection [6], the best way to detect a pulse of known shape (but unknown amplitude) over noise is to cross-correlate the signal with the function representing the pulse to detect. The cross-correlation is equivalent to a convolution with the time-reversed pulse (called the *matched filter*), therefore it can be computed as a FIR filtering. A N-tap FIR filter, however, requires N multiplications and N sums ($N = 17$ in our case); at the considered sample rate, this would require over $10^6\,\mathrm{multiplications/s}$, which is computationally unfeasible for the adopted computing hardware to be run in real time. For this reason, an approximated matched filter is considered, consisting of two rectangular windows (a 12-taps positive rectangle, a zero tap, and a 4-taps negative rectangle), as shown by the red line in Figure 4. Such a bi-rectangular FIR filter can be computed much more efficiently as a recursive filter. Referring to Figure 4, the output y_n (at time $t = nT_s$) of the bi-rectangular filtering can be expressed as follows:

$$\begin{aligned} y_n &= y_{1,n} + y_{2,n} \\ y_{1,n} &= y_{1,n-1} + A_1(x_n - x_{n-12}) \\ y_{2,n} &= y_{2,n-1} + A_2(x_{n-13} - x_{n-17}), \end{aligned}$$

where A_1 and A_2 are the amplitudes of the two rectangles. Combining the above equations yields

$$y_n = y_{n-1} + A_1(x_n - x_{n-12}) + A_2(x_{n-13} - x_{n-17})$$

whose computation requires just 2 multiplications and 4 sums per sample, allowing the proposed low-cost platform to compute the cross-correlation in real time.

A peak detection algorithm analyses the obtained cross-correlation signal. The algorithm detects a peaks each time the signal exceeds the detection threshold and remains above the threshold for at least 12 samples (corresponding to 324 µs). The threshold is adjusted dynamically, according to the current noise level; experimental results have shown the best behavior with a threshold y_{th} proportional to the 90$^{\text{th}}$ percentile of the noise floor, y_{90}. In particular, we got the best results setting $y_{th} = 1.05\ y_{90}$.

Each valid pulse recognized by the algorithm corresponds to a particle passing through the chamber, therefore the total intensity of the scattered light has to be estimated. As said before, in conditions of optimal detection, the peak value of the cross-correlation is proportional to the original amplitude of the detected pulse [6]. For this reason, the correlation peak value I_P is taken as measure of the total light intensity received by the photodiode. By exploiting the monotonic relationship between particle size and scattered light intensity described in Section II, it is possible to build a "calibration curve", which defines a bi-univocal correspondence between the measured peak amplitude I_P and the diameter of the particle that generated the light pulse.

The peaks are counted and grouped according to their amplitude. To this purpose, an array of counters is organized, each associated to an amplitude interval. Each counter works therefore as accumulation bin. At the end of a sampling session, the set of values in the counters represent the estimation of the amplitude distribution. A calibration of the system is now needed, in order to convert the peak amplitude distribution into a particle size distribution, that is the desired output of this instrument.

IV. Instrument Calibration

In order to obtain metrologically reliable granulometric measurements, the distribution of the peak values, as it is produced by the algorithm, has to be converted into the correct particle size distribution. It is therefore necessary to determine the relationship between a peak amplitude I_P and its corresponding particle size. We define this correspondence as the instrument calibration.

The best way to achieve this estimation would be to sample aerosols containing monodisperse particles, all having the same known size and refractive index. The instrument would detect the same peak intensity for all particles, thus providing the needed correspondence between intensity and size. However, monodispersed particles are very expensive and difficult to keep uniformly diffused in air (normally they are available in water solution). Conversely, there is a plenty of commonly-available sources of polydispersed particles for which, although the size of any single particle is unknown, their probabilistic size distribution is well known. For this reason, we propose a calibration procedure that makes use of commonly available polydispersed particulate. The underlying idea is that the scale factor to be calibrated can be determined as the value giving the best matching between the measured size distribution and the expected one.

We decided to employ talc powder, because its size distribution is known to be lognormal. A lognormal size distribution is common for many naturally or industrially generated particles, according to Kolmogorov's law of fragmentation [7]. For the adopted talc, the size distribution in weight is available from the manufacturer's product specifications [8], in terms of percentiles of the cumulated size distribution: $d_{50} = 8\ \mu\text{m}, d_{98} = 26\ \mu\text{m}$. This means that $99.7\%\ (\mu \pm 3\sigma)$ of the particles presents a size between $1.3\ \mu\text{m}$ and $47\ \mu\text{m}$. According to the analysis in Section II, for this range it is therefore reasonable to assume that $x \gg 1$, and, consequently, that the scattered intensity P_{Mie} is proportional to r^2. Considering the linear relationship between the peak amplitude I_P and P_{Mie}, we can therefore assume that:

$$I_P = \alpha \cdot r^2, \tag{1}$$

where α is the scale factor to calibrate.

In order to compare the output of the instrument with the known size distribution of the sample, we need a way to convert size distributions in weight into distributions of peak amplitudes. Considering the logarithm of the particle size, $r_{log} = \log(r)$, we can express the given size distribution of talc as normal distribution in r_{log}:

$$f_w(r_{log}) = \mathcal{N}(\mu_w, \sigma_w) \tag{2}$$

where $\mu_w = \log(d_{50})$ and $\sigma_w \approx \frac{\log(d_{98}) - \log(d_{50})}{2}$. The size distribution in weight can be converted to a size distribution in number of particles, as follows:

$$f_n(r) = \frac{\beta}{r^3} f_w(r) = \frac{\beta}{\sqrt{2\pi}\sigma_w} e^{-\frac{(\log(r)-\mu_w)^2}{2\sigma_w^2} - 3\log(r)};$$

after some mathematical steps, it can be shown that

$$f_n(r_{log}) = \mathcal{N}(\mu_n = \mu_w - 3\sigma_w^2\ ,\ \sigma_n = \sigma_w), \tag{3}$$

which is still a lognormal distribution, with the same standard deviation as $f_w(r_{log})$, but a different mean.

We can now obtain the distribution of the peak amplitudes corresponding to $f_n(r_{log})$ by considering equation (1) expressed in logarithmic form:

$$\log(I_P) = \log(\alpha) + 2r_{log}. \tag{4}$$

Due to the linear relationship between r_{log} and $\log(I_P)$, we obtain

$$f\left(\log(I_P)\right) = \mathcal{N}\left(\mu_I = \log(\alpha) + 2\mu_n\ ,\ \sigma_I = 2\sigma_n\right). \tag{5}$$

From equation (5) we can derive that:

- the distribution of the peak amplitude is also lognormal;

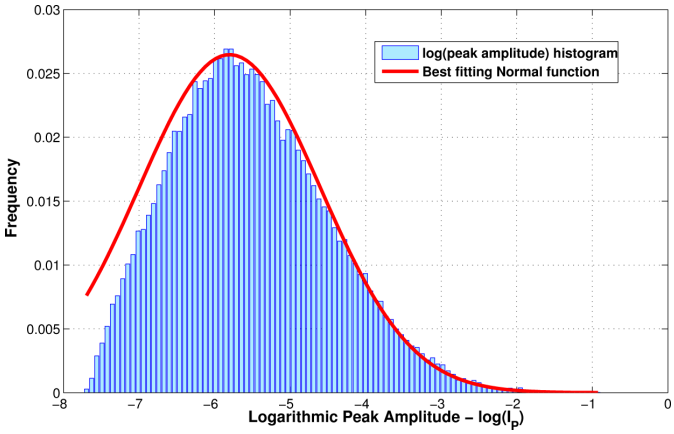

Fig. 5. The bars represent the histogram of the measured peak amplitudes, as $\log(I_P)$, for the talc sample. The red line represents the best fitting normal distribution ($\mu_I = -5.75$, $\sigma_I = 1.20$).

- the standard deviation $\sigma_I = 2\sigma_n = 2\sigma_w$. This means that, for lognormally distributed particulate, no calibration is necessary to estimate the particle size variance;
- the mean:

$$\mu_I = \log(\alpha) + 2\mu_n = \log(\alpha) + 2\mu_w - 6\sigma_w^2 \qquad (6)$$

allows us to estimate α, thus calibrating the instrument, as:

$$\alpha = \exp\left(\mu_I - 2\mu_w + 6\sigma_w^2\right).$$

A. Experimental results

As said before, the distribution parameters of the talc powder are provided in the manufacturer's product specifications [8] in terms of percentiles in weight. The mean and standard deviation of the size distribution in weight can be derived as:

$$\begin{aligned} \mu_w &= \log(d_{50}) = \log(8\ \mu\text{m}) = 2.079\ \log(\mu\text{m}) \\ \sigma_w &\approx \frac{\log(d_{98}) - \log(d_{50})}{2} = 0.589\ \log(\mu\text{m}) \end{aligned}$$

and, using equation (3), the size distribution in number as:

$$\begin{aligned} \mu_n &= \mu_w - 3\sigma_w^2 \approx 1.038\ \log(\mu\text{m}), \\ \sigma_n &= \sigma_w \approx 0.589\ \log(\mu\text{m}). \end{aligned}$$

We let the instrument sample air in which the talc powder was diffused. Figure 5 reports the histogram of $\log(I_P)$ produced by the instrument, which confirms the actual lognormal distribution of the peak amplitudes. A normal function was fitted over the empirically obtained distribution, taking care of the fact that the distribution is partially truncated on the left, due to the sensitivity limit of the instrument. The maximum-likelihood normal function which best fits the distribution is represented by the solid red line in Figure 5, with mean $\mu_I = -5.75$ and standard deviation $\sigma_I = 1.20$.

The obtained experimental value for σ_I differs therefore from the expected one, $\sigma_I = 2\sigma_n \approx 1.179\ \log(\mu\text{m})$, by just 1.7%, a really encouraging result.

Finally, the calibration parameter α could be determined using equation (6):

$$\log(\alpha) = \mu_I - 2\mu_n \approx -7.825\ \log(\mu\text{m}^{-2})$$

yielding:

$$\alpha \approx \exp(-7.825) = 4.00 \cdot 10^{-4}\ \mu\text{m}^{-2}.$$

It is difficult to provide by computation a reliable evaluation of the accuracy of this calibration. The confidence intervals on the estimation of α, provided by the χ_{N-1} function, would show that the accuracy could be arbitrarily enhanced by increasing the number of sampled particles N, that is, just sampling for longer times. However, the accuracy of this calibration is more significantly limited by the introduced simplifying assumptions, like the reduction of the relationship between scattered intensity and particle radius, plotted in Fig. 1, to the simple equation (1), and by other sources of uncertainty, like the unknown shape and refraction index of the sampled particles.

V. Conclusion

This work has shown the feasibility of an instrument for particle size analysis characterized by low hardware cost and simplicity of calibration.

The obtained experimental results show promising performances, particularly in terms of size resolution, but show that still some effort is needed to improve the detection sensitivity, in order to lower the size of the smallest detectable particle. Further research will be carried out in order to enhance the detection sensibility and to improve the calibration procedure, by considering currently neglected aspects (like the particles' refraction index) and by introducing a more accurate modelling of the relationship between scattered intensity and particle radius.

References

[1] H.C. Hulst, *Light scattering by small particles*. Dover Publications, 1981.
[2] G. Lonati and M. Giugliano, Size distribution of atmospheric particulate matter at traffic exposed sites in the urban area of Milan (Italy), *Atmospheric Environment*, 40:264–274, 2006.
[3] G. Mie, Beiträge zur Optik trüber Medien, speziell kolloidaler Metallösungen, *Annalen der Physik*, 25:377–445, 1908.
[4] G.W. Petty, *A First Course In Atmospheric Radiation*. Sun Dog Books, 2nd edition, 2006.
[5] A. Tittarelli, A. Borgini, M. Bertoldi, E. DeSäger, A. Ruprecht, R. Stefanoni, G. Tagliabue, P. Contiero, and P. Crosignani, Estimation of particle mass concentration in ambient air using a particle counter. *Atmospheric Environment*, 42(36):8543–8548, 2008.
[6] S. Haykin, *Communication Systems*. John Wiley & Sons, 3 edition, 1994.
[7] A. N. Kolmogorov, On the logarithmically normal distribution law of particle sizes at the subdivision, *Doklady Akademii Nauk SSSR* 31, no. 2, 99–101, 1941.
[8] Mondo Minerals B.V., *Low Oil Absorption Talc for High Solids Coatings*, Technical Bullettin 1206, http://www.mondominerals.com/-uploads/media/Mondo_TB1206.pdf
[9] U.S. Environmental Protection Agency, *National Ambient Air Quality Standards (NAAQS)*, http://epa.gov/air/criteria.html